Z. Phys. B – Condensed Matter 83:273–276 (1991)

Condensed Matter
Zeitschrift für Physik B

Phase diagram of the ANNNI model in the Hamiltonian limit *

C.M. Arizmendi[1], A.H. Rizzo[1], L.N. Epele[2], and C.A. García Canal[2]

[1] Facultad de Ingeniería, Universidad Nacional de Mar del Plata, J.B. Justo 4302, 7600 Mar del Plata, Argentina
[2] Laboratorio de Física Teórica, Departamento de Física, Universidad Nacional de La Plata, C.C. 67, 1900 La Plata, Argentina

Received July 3, 1990; revised version December 12, 1990

The Hamiltonian limit of the ANNNI model in $(1+1)$ dimensions is studied by using the Quantum Statistical Monte Carlo method. Even if recent results suggest that Monte Carlo calculations may prove unreliable in the study of this system, the phase diagram of the quantum version of the model was successfully obtained. In particular, the elusive transitions between the disordered, the floating incommensurate and the degenerate $\langle 2, 2\rangle$ are determined by analysing the correlation length behaviour in finite lattices.

The numerical analysis of the critical properties of quantum spin Hamiltonians can be carried out using essentially two alternative methods. One of them consists in the direct simulation of the quantum system [1] while the other one exploits the equivalence of the original problem with an adequate classical system [2].

In this paper we present the study of the ANNNI model [3] performed by using the second alternative above. We are particularly interested in the quantum ANNNI model because it implies competing interactions between first and second neighbours and displays several interesting physical features. We could mention for example the presence of: modulated magnetic structures, incommensurate-commensurate transitions, a multicritical point, a Lifshitz point and a disorder line. Notice that the ANNNI Hamiltonian is useful in understanding systems that present sinusoidal magnetic order as for erbium and other rare earth elements. It could also be related to cerium antimonide which exhibits ordered magnetic layers with periods commensurate with the lattice [4].

This model with competing interactions has been intensively studied in the literature, in particular, its one dimensional quantum version [5–7] and its classical Hamiltonian in two and three dimensions. For a recent review see [5].

* Partially supported by CONICET Argentina

We have carefully analysed the phase diagram of the quantum ANNNI model in 1-dimension by means of the so called Quantum Statistical Monte Carlo Method [2]. For this purpose we have used the equivalence, via the Trotter formula, between the model of interest and the corresponding 2-dimensional anisotropic classical system.

It should be mentioned that there exists a quite long controversy with respect to the present system. In fact, previous results [8] suggested that numerical methods, such as Monte Carlo and Transfer Matrix, were unreliable, but later the scaling transfer matrix [6] and a dynamical Monte Carlo [7] have produced good results. We have, in some sense, clarified this controversial situation: we have found that both the correlation function and the correlation length obtained by Monte Carlo techniques, allow us to distinguish correctly the disordered and floating incommensurate phases of the model (called floating fluid and floating solid by some authors [6]). In general we have obtained the full phase diagram of the $(1+1)$ ANNNI model that agrees very well with some exact [9] and recent numerical results [6, 7, 10].

Quantum statistical Monte Carlo method

We briefly sketch here the appropriate numerical technique for the study of quantum statistical problems, which has been used in solving the ANNNI model. It is based on the Trotter formula which allows one to establish the equivalence between the partition function corresponding to a d-dimensional quantum system and that of a $d+1$-dimensional classical one [2].

Let the partition function for the quantum ANNNI model in a lattice of 1 dimension and N sites be

$$\mathscr{Z} = \mathrm{Tr}\left\{\exp\left[\beta \sum_{i=1}^{N} (J, A_i + J_2 B_i + \Gamma C_i)\right]\right\} \tag{1}$$

with

$$A_i = \sigma_i^z \sigma_{i+1}^z; \quad B_i = \sigma_i^z \sigma_{i+2}^z; \quad C_i = \sigma_i^x \tag{2}$$

and where as usual $\sigma_i^{\alpha}(\alpha = z, x)$ are the standard Pauli matrices representing the spin operator at the site i.

We use now the Trotter formula, which in its simplest version and for any operators O_1 and O_2 reads

$$\exp(O_1+O_2)=\lim_{m\to\infty}(\exp(O_1/m)\exp(O_2/m))^m \tag{3}$$

in order to factorize the partition function in the form:

$$\mathscr{Z}=\lim_{m\to\infty}\mathscr{Z}_m \tag{4}$$

where clearly

$$\mathscr{Z}_m=\mathrm{Tr}\left\{\exp\left[\beta/m\sum_{i=1}^{N}(J_1 A_i+J_2 B_i)\right]\exp\left[\frac{\beta\Gamma}{m}\sum_{i=1}^{N}C_i\right]\right\}^m. \tag{5}$$

Being interested in the ground state properties of the model one has to study its behaviour at temperature $T=0$. This limit is conveniently obtained by considering the parameter $n(=\beta\Gamma)\to\infty$ by integer values such that

$$\mathscr{Z}=\lim_{\substack{m\to\infty\\ n\to\infty}}\mathscr{Z}_{mn} \tag{6}$$

with

$$\mathscr{Z}_{mn}=\mathrm{Tr}\left\{\left[\exp\left(\frac{J_1}{m\Gamma}\sum_{i=1}^{N}A_i\right)\exp\left(\frac{J_2}{m\Gamma}\sum_{i=1}^{N}B_i\right)\exp\left(\frac{1}{m}\sum_{i=1}^{N}Ci\right)\right]^{mn}\right\}. \tag{7}$$

We use, next, the identity

$$\left\langle S\left|\exp\left(\frac{\sigma^x}{m}\right)\right|s'\right\rangle=\left[\frac{1}{2}\sinh\left(\frac{2}{m}\right)\right]^{1/2}\exp\left\{\frac{ss'}{2}\ln\left[\coth\left(\frac{1}{m}\right)\right]\right\} \tag{8}$$

with

$$\sigma^z|s\rangle=\pm|s\rangle \tag{9}$$

after inserting the complete set of states $|s\rangle$ in Eq. (7). In this way one obtains, for m and n sufficiently large, an approximation to the quantum partition function (1) that reads

$$\mathscr{Z}_{mn}=\left[\frac{1}{2}\sinh\left(\frac{2}{m}\right)\right]^{\frac{N_{mn}}{2}}\mathrm{Tr}\{\exp(H_c)\}, \tag{10}$$

where

$$H_c=\sum_{i=1}^{N}\sum_{j=1}^{mn}\left\{\frac{J_1}{m\Gamma}s_{ij}s_{i+1\,j}+\frac{J_2}{m\Gamma}s_{ij}s_{i+2\,j}+J_3\,s_{ij}s_{ij+1}\right\},$$

with

$$J_3=\tfrac{1}{2}\ln\left[\coth\left(\frac{1}{m}\right)\right]. \tag{11}$$

The Monte Carlo simulation is now performed with this classical model. It is defined on a square lattice having N horizontal spins and mn vertical spins as sketched in Fig. 1. Periodic boundary conditions were used. Notice that mn is the so called Trotter dimension.

Our equivalent classical two-dimensional system is not exactly the same as the standard classical problem usually considered. In fact, the case under consideration implies in general an anisotropy in the sense that the first neighbours interacting in the original direction are driven by a different coupling than the equivalent neighbours in the Trotter direction (see Fig. 2).

The numerical analysis was carried out by using the standard Metropolis algorithm [11]. The lattice size was varied between 60 and 200 sites in the horizontal direction and between 30 and 70 in the vertical one. The

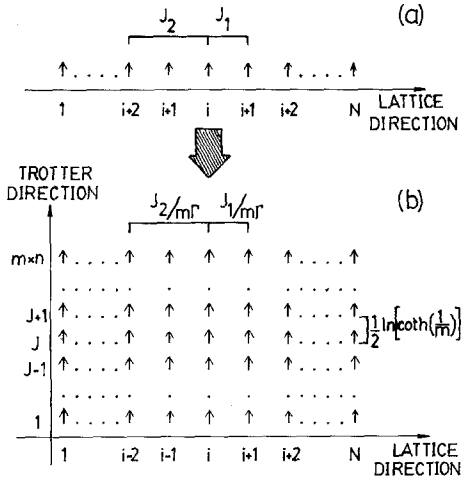

Fig. 1. Equivalence between the quantum (1+1) dimensional **a** and the classical (2)-dimensional **b** models. Both models have N spins in the direction where competing interactions are present and the classical one has $m.n$ spins in the Trotter direction

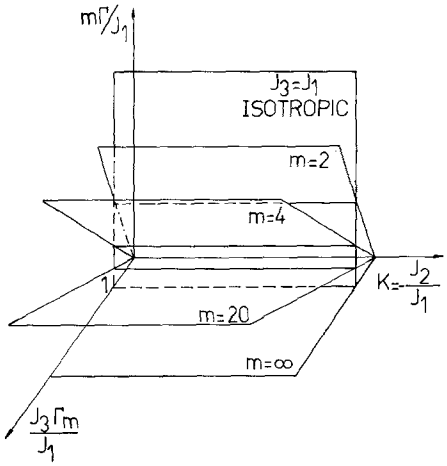

Fig. 2. Axis for the phase diagram. The standard classical diagram corresponds to $J_3=J_1$. The exact quantum map is for m and $n\to\infty$

results here reported correspond to a Trotter index $m=6$ because other cases as $m=4$, $m=8$ and $m=10$ do not present significant qualitative differences. So we considered that the thermalization of the system is reached after 3×10^3 to 10^4 Monte Carlo steps per spin (MCS). On the other hand, the pertinent averages were evaluated with 2.5×10^4 to 10^5 MCS. All the calculations were done using two different starting configurations, namely, a ferromagnetic one for values of $K=-J_2/J_1<0.5$ and a degenerate one $[\langle 2\rangle-(\uparrow\uparrow\downarrow\downarrow\ldots\uparrow\uparrow\downarrow\downarrow)]$ for the rest. Notice that the results are insensitive to the use of a completely disordered starting configuration.

In order to simplify the presentation of the results, it was decided to deal with the classical magnitudes, which are proportional to the equivalent quantum ones [2]. The magnitudes that were explicitly considered are: the energy E, the horizontal correlation function $\langle s_{00}\, s_{0+\pi_0}\rangle-\langle s_{00}\rangle\langle s_{0+\pi_0}\rangle$ and the vertical one $\langle s_{00}\, s_{00+\pi}\rangle-\langle s_{00}\rangle\langle s_{00+\pi}\rangle$ together with its correlation lengths $\zeta^{\parallel}$, $\zeta^{\perp}$ were also analysed.

Phase diagram

The full phase diagram obtained in the present calculation is shown in Fig. 3. The lines there were drawn to guide the eye and some of the computed points are explicitly reported together with the statistical errors. The phase plane structure needs the following comments:

a) Ferromagnetic-paramagnetic transition line. This line separates the regions 1 and 2 of the phase diagram. It was obtained finding the position of both the vertical and the horizontal correlation length.

The position of this line agrees very well with an analytic expression of the phase boundary obtained by the method of Müller-Hartmann and Zittartz (MH-Z) [5, 12]. The boundary is obtained in the MH-Z approximation for $K=-J_2/J_1<0.5$ from the equation

$$\sinh\left[2\left(\frac{J_1}{m\Gamma}+2\frac{J_2}{m\Gamma}\right)\right]\sinh 2J_3=1, \tag{12}$$

for the m-approximation to the quantum ANNNI model. This method is believed to give quite accurate but no exact estimates for the phase boundaries

b) Disorder line (DOL) *and one dimensional line* (ODL). The ODL can be obtained analytically [9]. It is inside the disorder region and ends at the multicritical point ($\Gamma/J_1=0$; $K=0.5$). The line displayed in Fig. 3 near the ferromagnetic – paramagnetic transition corresponds to the analytical ODL. The presence of this line avoids the existence of a Lifshitz point in the ferromagnetic border line.

Our calculation detects this line through the minimum in the horizontal correlation length. A characteristic correlation length behaviour is shown in Fig. 4. The numerical results obtained agree very well with the analytical ODL as can be seen in Fig. 3.

The ANNNI model must also have a line that separates the fluid phase 2, where the horizontal correlation function behaves as $\exp(-r/\zeta^{\parallel})$, from the disordered incommensurate phase 3 where that function behaves as $\exp(-r/\zeta^{\parallel})\cos(q\cdot r)$. This line is called disorder line (DOL) [9, 13]. Evidently, the transition between these two phases could be identified by detecting the vanishing of q. The above mentioned change of behaviour of the horizontal correlation function across the DOL is exhibited in Fig. 5.

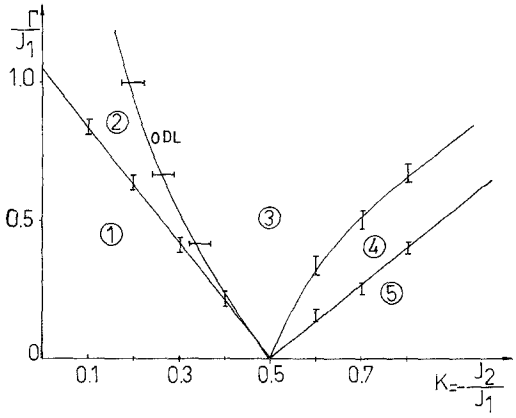

Fig. 3. Full phase diagram of the (1 + 1)-dimension quantum ANNNI model. Phases: 1 – Ferromagnetic, 2 – Fluid, 3 – Disordered, 4 – Floating incommensurate, 5 – Degenerate $\langle 2\rangle$. This phase diagram was obtained with the $m=6$, $n=10$ approximation. This was chosen as a good approximation because other values of m, n do not present significative differences. The analytical ODL is also indicated

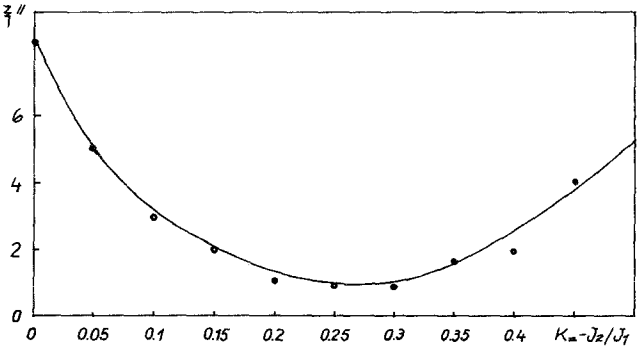

Fig. 4. Horizontal correlation length for $\Gamma/J_1=1.20$ showing a minimum for the range $0.2\leqq K\leqq 0.3$

The differences between the results presented here and the theoretical expectations are due to the finite size of the lattice. Figure 5a, b are similar in the sense that they do not present zeros. This corresponds to a $q=0$ value and for that reason the oscillations in Fig. 5b are different from those in Fig. 5c or d. We find that by increasing the lattice dimension the oscillations of Fig. 5b decrease and it becomes like Fig. 5a, which means that these oscillations are higher order effects due to the proximity of the second neighbour interaction zone.

We could detect the ODL through the minimum of the correlation length and the DOL through the correlation function. These two lines cannot be clearly differentiated numerically. For that reason the error bars around the analytical ODL indicate both the ODL and the DOL simulation results.

c) Disordered – floating incommensurate-$\langle 2\rangle$*-transitions.* The determination of the critical lines between regions 3,

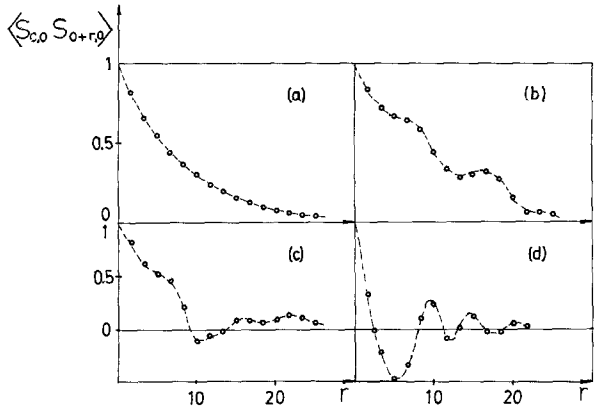

Fig. 5a–d. Correlation function behaviour when going through the disorder line (DOL) for $\Gamma/J_1 = 1.2$. **a** net fluid phase: $K = 0$; **b** fluid phase nearer the DOL: $K = 0.10$; **c** disordered phase immediately after the DOL: $K = 0.25$; **d** net disordered phase: $K = 0.5$

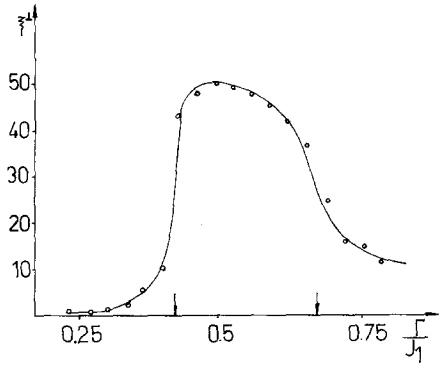

Fig. 6. Vertical correlation lengths behaviour in the disordered-floating incommensurate-$\langle 2 \rangle$ transition showing the effect for $K = 0.8$. The corresponding transition points are indicated by the arrows and they occur when $\zeta^{\perp}(K) = m.n. = 30$, the vertical dimension

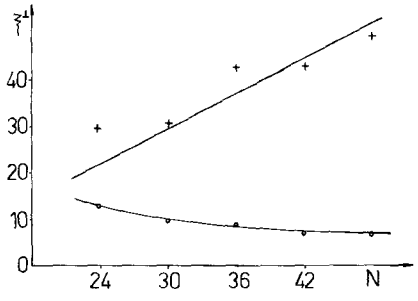

Fig. 7. Finite size scaling results for the vertical correlation function as a function of the lattice size in the Trotter direction: ∘∘∘ disordered phase; + + + floating incommensurate phase. Lines are for guiding the eyes

4 and 5 of the phase plane is the most elusive one because it implies to numerically distinguish between an exponential and a power decay in the behaviour of the correlation function. Moreover, the behaviour, expected in the thermodynamic limit, is masked in the present case of a finite lattice for an exponential. For this reason, the distinction between both phases implies the distinction between two different correlation lengths driving the corresponding exponentials. In the disordered phase and in the $\langle 2 \rangle$ phase, this length has a finite value while in the floating incommensurate, being a critical zone [10] it diverges. This expected divergence manifests itself in finite lattice calculations when the correlation length approaches the size of the lattice. This fact is clearly seen in the examples of Fig. 6. It is important to stress that we calculated the vertical correlation function because in this Ising-like direction thermalization problems are avoided.

Another test of the above conclusions is given by the analysis of the correlation length when the vertical dimension is changed. In the disordered phase it remains constant while in the floating incommensurate phase it increases proportionally to the lattice size. This is shown in Fig. 7.

Summary

The entire phase diagram of the quantum $(1+1)$ dimension ANNNI model has been obtained by Monte Carlo simulation techniques. The present analysis clearly shows the existence of a disorder line (DOL) and a one-dimensional line (ODL) in agreement with the analytical predictions [9]. This goal ensures a phase configuration without conflict with exact calculations. On the other hand, the differentiation between the disordered, the floating incommensurate, and the $\langle 2 \rangle$ phases has been successfully coped by the analysis of the correlation length. This technique seems to be well adapted for studying similar situations in other spin systems, specially those with competing interactions.

We would like to emphasize that it was possible to determine the phase-diagram by using the vertical correlation function behaviour. In this way we were able to avoid the thermalization problems related with competing interactions in the horizontal direction. In any case, all the necessary checks were performed.

We warmly acknowledge helpful comments of H. Ceva, H. Fanchiotti and S. Sciutto. C.A. Garcia Canal acknowledges the J.S. Guggenheim foundation for a fellowship.

References

1. See for example Epele, L.N., Fanchiotti, H., Garcia Canal, C.A., Sciutto, S.J.: J. Comput. Phys. **77**, 79 (1989)
2. Suzuki, M.: Prog. Theor. Phys. **56**, 1454 (1976); J. Stat. Phys. **46**, 883 (1986)
3. Elliott, R.J.: Phys. Rev. **124**, 346 (1961)
4. Habenschuss, M., Stasses, C., Sinha, S.K., Deckmann, H.W., Speeding, F.H.: Phys. Rev. B **10**, 1021 (1974); Fisher, P., Lebeck, B., Meier, G., Rainford, B.D., Vogt, O.: J. Phys. C **11**, 345 (1978)
5. Selke, W.: Phys. Rep. **170**, 213–264 (1988)
6. Beale, P., Duxbury, P., Yeomans, J.: Phys. Rev. B **31**, 7166 (1985); Grynberg, M.D., Ceva, H.: Phys. Rev. B **36**, 7091 (1987)
7. Barber, M.N., Derrida, B.: J. Stat. Phys. **51**, 877 (1988)
8. Morgenstein, I.: Phys. Rev. B **29**, 1458 (1984)
9. Peschel, I., Emery, V.J.: Z. Phys. B – Condensed Matter **43**, 241 (1981)
10. Finel, A., Fontaine, D. de: J. Stat. Phys. **43**, 645 (1986)
11. Metropolis, N., Rosenbluth, A.W., Rosenbluth, M.N., Teller, A.H., Teller, E.: J. Chem. Phys. **21**, 1087 (1953)
12. Müller Hartmann, E., Zittartz, J.: Z. Phys. B – Condensed Matter and Quanta **27** 261 (1977)
13. Rujan, P.: J. Stat. Phys. **29**, 231 (1982)